

Dynamical and spectral decompositions of the generalized friction tensor for optimal control

Jordan R. Sawchuk* and David A. Sivak†

Department of Physics, Simon Fraser University, Burnaby, British Columbia, Canada V5A1S6

(Dated: September 27, 2024)

Optimal control of stochastic systems plays a prominent role in nonequilibrium physics, with applications in the study of biological molecular motors and the design of single-molecule experiments. The optimization problem rarely admits exact analytic solutions, but under slow driving it can be recast geometrically solely in terms of equilibrium properties. Minimum-work protocols are geodesics on a thermodynamic manifold whose metric is a generalized friction tensor. Here we derive two decompositions of a full-control friction tensor that assumes total control over the potential energy. Arbitrary conservative-control friction tensors are then inherited metrics on hypersurfaces of constraint. Our reformulation simplifies the derivation of friction tensors for many systems and provides design principles for optimal control. This approach gives insight into the domain of applicability of the friction-tensor formalism by demonstrating explicitly how minimum-work protocols take advantage of multi-exponential relaxation to increase accuracy.

I. INTRODUCTION

A central question in nonequilibrium thermodynamics concerns the “price of haste” [1]. During a quasistatic (or infinite-duration) process where a system remains at equilibrium, thermodynamic quantities like total dissipation depend only on the initial and final states; however, when external driving is fast with respect to internal system dynamics or energy scales are comparable to thermal fluctuations, well-established results from equilibrium thermodynamics no longer apply: instantaneous values of macroscopic observables fundamentally depend on the history of the system, and for microscopic systems like molecular machines, these quantities are stochastic, with protocol-dependent distributions [2]. These factors present challenges to uncovering universal principles governing many systems of theoretical and practical interest, such as biological molecular motors which operate in the nonequilibrium environment of living cells—often with remarkable speed and efficiency [3].

Optimal control theory is one framework for navigating the complexity of nonequilibrium statistical physics: given a cost function and boundary conditions, optimization selects a set of privileged paths from the uncountable infinity of thermodynamically distinct paths in control-parameter space. The excess work—the extra energy required to drive a process in finite time—is a commonly studied cost function [4]. Minimum-work protocols (MWP) minimize the ensemble average of the excess work.

Although analytic solutions exist for some simple systems [5–7], the general problem is intractable. Reformulating the optimal-control problem as a system of Hamiltonian equations allows for the application of numerical methods for ordinary differential equations [6]; however,

computation rapidly becomes prohibitively expensive for large systems, high-dimensional control vectors, or systems driven near a critical point. Ongoing efforts to address these challenges include methods employing machine learning [8].

An alternative approach is to apply suitable approximations that simplify the optimal control problem. Under the assumption of sufficiently slow driving, the friction-tensor formalism expresses the excess work purely in terms of equilibrium information [9]. Within this approximation’s domain of applicability, MWPs may be interpreted as geodesics on a thermodynamic manifold whose intrinsic geometry is described by a generalized friction tensor.

The friction-tensor formalism has been applied in various contexts, including the study of driven barrier crossings as a model of single-molecule force-extension experiments [10], driving the biological rotary motor F_1 ATPase [11, 12], folding of DNA hairpins [13], control of protein copy-number distributions [14], bounds on the efficiency of membrane separation of binary gases [15], and nonequilibrium phase transitions [16]. The formalism has also been extended beyond the classical regime to quantum systems [17]. A re-weighted friction tensor has been introduced for the efficient sampling of free-energy surfaces [18] with applications to the binding affinity of drugs [19].

In this work, we introduce a reformulation of the friction-tensor formalism for conservative control of systems with discrete spectra. After reviewing the friction-tensor formalism, we define a full-control friction tensor (22) by assuming arbitrary control over the potential energy. For discrete systems, we derive two decompositions (30, 45) of the full-control friction tensor that facilitate both interpretation and calculation of the friction landscape and MWPs and demonstrate the approach through simple examples. We then show that analogous decompositions (52, 54) hold for continuous systems with discrete spectra. For parametric control governed by a set of control parameters, we show that the friction tensor

* jordan.sawchuk@sfu.ca

† dsivak@sfu.ca

is an inherited metric on a submanifold. The full-control friction tensor is thus shown to define a global thermodynamic geometry from which all other friction tensors for conservative driving may be derived. We provide insight into the accuracy of the friction-tensor formalism by deriving a spectral decomposition of the nonlinear-response contributions to the excess power (101). This result explains the observation that the friction-tensor formalism performs well beyond the expected regime [20] by demonstrating how systems can remain near equilibrium for fast protocols by taking advantage of multi-exponential relaxation. The decomposition further provides a natural route to derive higher-order corrections (104) to the linear-response approximation.

II. PRELIMINARIES

Throughout, we consider continuous-time Markov processes X_t on a state space Ω which may be either discrete or continuous. For a continuous state space, we remain agnostic about the dimension of states $x \in \Omega$. When Ω is discrete, we choose some canonical ordering of the states such that state functions g may be written as $g(s_i) = g_i$ for $i = 0, 1, 2, \dots$. We often write discrete state functions as vectors $\mathbf{g} \in \mathbb{R}^{|\Omega|}$. We use the notation $g(s)$ with no index on s when we don't disambiguate between continuous and discrete Ω .

The probability distribution of a system at time t is represented by the vector $\mathbf{p}(t)$ for discrete systems and by the function $p(x, t)$ for continuous systems. The time-evolution of the probability distribution is governed by an infinitesimal generator, defined by the $|\Omega| \times |\Omega|$ matrix \mathbb{W} for discrete systems and by the linear operator \mathcal{L} for continuous systems. The master equation

$$\frac{d\mathbf{p}(t)}{dt} = \mathbb{W}\mathbf{p}(t) \quad (1)$$

governs the evolution of $\mathbf{p}(t)$, and the Fokker-Planck equation

$$\frac{\partial p(x, t)}{\partial t} = (\mathcal{L}p)(x, t) \quad (2)$$

governs the evolution of $p(x, t)$.

Here we consider generators with a discrete spectrum and a unique stationary distribution π . We denote the eigentriples as $(-\lambda_j, \psi^{(j)}, \phi^{(j)})$ such that on discrete state spaces

$$\mathbb{W}\psi^{(j)} = -\lambda_j\psi^{(j)} \quad (3a)$$

$$\mathbb{W}^T\phi^{(j)} = -\lambda_j\phi^{(j)} \quad (3b)$$

and on continuous state spaces

$$\mathcal{L}\psi^{(j)} = -\lambda_j\psi^{(j)} \quad (4a)$$

$$\mathcal{L}^\dagger\phi^{(j)} = -\lambda_j\phi^{(j)}, \quad (4b)$$

for adjoint \mathcal{L}^\dagger . The eigenvalues are ordered as $\lambda_0 < \lambda_1 \leq \dots$, so that $(\lambda_0, \psi^{(0)}, \phi^{(0)}) = (0, \pi, 1)$. We will use π and $\psi^{(0)}$ interchangeably to refer to the equilibrium distribution.

The eigenfunctions form dual bases and are normalized such that

$$\langle \psi^{(i)}, \phi^{(j)} \rangle = \delta_{ij}, \quad (5)$$

for Kronecker delta δ_{ij} . $\langle \cdot, \cdot \rangle$ denotes the Euclidean inner product when the arguments are vectors and the L^2 inner product when the arguments are functions:

$$\langle \psi^{(i)}, \phi^{(j)} \rangle \equiv \begin{cases} \sum_{s \in \Omega} \psi^{(i)}(s) \phi^{(j)}(s) & \Omega \text{ discrete} \\ \int_{\Omega} \psi^{(i)}(s) \phi^{(j)}(s) ds & \Omega \text{ continuous.} \end{cases} \quad (6)$$

Denote by \mathbf{u} a set of m external control parameters whose time evolution $\mathbf{u}(t)$ is deterministic. Given some cost functional \mathcal{C} , an optimal control protocol is a function $\mathbf{u}^* : [0, \tau] \rightarrow \mathbb{R}^m$ satisfying

$$\mathbf{u}^* = \underset{\mathbf{u}}{\operatorname{argmin}} \{ \mathcal{C}[\mathbf{u}] \}, \quad (7)$$

subject to an appropriate set of boundary conditions and supplemental constraints.

The choice of cost function will depend on the context: e.g., one may wish to minimize entropy production or the loss of available work, maximize power output or efficiency, or optimize some linear combination of these [1, 21]. Here we consider the average excess work, defined to be the work done in excess of the equilibrium free-energy difference $F(\mathbf{u}(\tau)) - F(\mathbf{u}(0))$.

We assume conservative control in which driving may be expressed by a time-dependent potential energy $V(t)$ [22]. For parametric control, this time-dependence arises through the control parameters \mathbf{u} , i.e., $V(t) = V(\mathbf{u}(t))$. In this case, for fixed \mathbf{u} the equilibrium distribution is the Boltzmann distribution

$$\pi(s; \mathbf{u}) = e^{-\beta[V(s; \mathbf{u}) - F(\mathbf{u})]}, \quad (8)$$

for free energy $F(\mathbf{u})$.

The vector of generalized forces conjugate to the control parameters \mathbf{u} is

$$\mathbf{f} \equiv -\nabla_{\mathbf{u}} V. \quad (9)$$

The average excess work is

$$\langle \mathcal{W}_{\text{ex}} \rangle = - \int_0^\tau dt \frac{d\mathbf{u}^T}{dt} \langle \delta \mathbf{f} \rangle_{p(t)}, \quad (10)$$

where $\delta \mathbf{f} = \mathbf{f} - \langle \mathbf{f} \rangle_\pi$ is the deviation of \mathbf{f} from its average with respect to the equilibrium distribution π , and $\langle \cdot \rangle_{p(t)}$ denotes an average with respect to the solution of the master equation (1) with $\mathbb{W}(t) = \mathbb{W}(\mathbf{u}(t))$ or the Fokker-Planck equation (2) with $\mathcal{L}(t) = \mathcal{L}(\mathbf{u}(t))$.

III. RIEMANNIAN GEOMETRY OF OPTIMAL CONTROL

The nonequilibrium average in (10) presents a significant challenge to obtaining exact MWPs. The friction-tensor formalism simplifies the optimization problem by expressing the excess work in terms of equilibrium quantities alone. This approximation gives rise to a metric for a thermodynamic manifold on which distances represent the excess work for near-equilibrium driving.

In this section, we review the friction-tensor formalism, following the original derivation [9], but there exist several other distinct derivations. The so-called derivative truncation approximation [23] expands the deviation $\delta p(x, t)$ of the probability density in a small parameter ϵ that sets the relative dynamical timescales of the system and the control protocol. While this approach clarifies the domain of applicability of the linear-response approximation for one-parameter control of continuous systems, it is not clear how to apply the same analysis to discrete-state systems or to multi-parameter control. Methods from adiabatic perturbation theory have been applied to derive analogous results [24]. Finally, an expansion of $\delta p(x, t)$ in powers of a particular operator leads to the same results [25]. The latter approach provided significant inspiration for the work in Section IV.

The excess power during a protocol \mathbf{u} is the integrand appearing in the excess work (10):

$$\langle \mathcal{P}_{ex}(t) \rangle = -\frac{d\mathbf{u}^T}{dt} \langle \delta \mathbf{f} \rangle_{p(t)}. \quad (11)$$

If the system remains close to equilibrium throughout the driving process, dynamic linear response approximates the average deviation of the conjugate forces as

$$\langle \delta \mathbf{f} \rangle_{p(t)} \approx \int_{-\infty}^t dt' \chi(t-t') [\mathbf{u}(t') - \mathbf{u}(t)], \quad (12)$$

where

$$\chi(t) = \beta \frac{d\Sigma(t)}{dt} \equiv \beta \frac{d}{dt} \langle \delta \mathbf{f}(t) \otimes \delta \mathbf{f}(0) \rangle_{\pi(\mathbf{u}(t))} \quad (13)$$

represents the system response at time t to a perturbation of the control parameters at time 0. The symbol \otimes denotes the outer (or dyadic) product: $[\mathbf{v} \otimes \mathbf{w}]_{ij} = v_i w_j$.

Under the assumption that the driving is slow compared to the system's relaxation timescales,

$$\langle \delta \mathbf{f} \rangle_{p(t)} \approx \left[\int_0^\infty dt \Sigma(t) \right] \frac{d\mathbf{u}}{dt}. \quad (14)$$

Defining the generalized friction tensor as

$$\zeta(\mathbf{u}) \equiv \beta \int_0^\infty dt \langle \delta \mathbf{f}(t) \otimes \delta \mathbf{f}(0) \rangle_{\pi(\mathbf{u})}, \quad (15)$$

we obtain the linear-response approximation of the excess work

$$\langle \mathcal{W}_{ex} \rangle^{LR} = \int_0^\infty dt \frac{d\mathbf{u}^T}{dt} \zeta(\mathbf{u}(t)) \frac{d\mathbf{u}}{dt}. \quad (16)$$

The component $\zeta_{ij}(\mathbf{u})$ of the generalized friction tensor thus approximates how the energy cost of simultaneously changing the control parameters u_i and u_j varies with the velocity of the control parameters. In the approximation's domain of applicability, this scaling is set by the integrated equilibrium time-correlation of the conjugate-force deviations, at a fixed value of the control parameters.

The generalized friction tensor is positive-definite and symmetric, so the linear-response excess work (16) is the energy functional of a curve on a thermodynamic manifold \mathcal{M} with intrinsic geometry described by the Riemannian metric tensor ζ [26]. Geodesics on \mathcal{M} are minimum-work protocols, obtained by solving the geodesic equations [27]

$$\frac{d^2 u^i}{dt^2} + \sum_{j,k} \Gamma^i_{jk} \frac{du^j}{dt} \frac{du^k}{dt} = 0, \quad i = 1, \dots, m, \quad (17)$$

for Christoffel symbols of the second kind

$$\Gamma^i_{jk} \equiv \frac{1}{2} \sum_\ell \zeta^{i\ell} \left(\frac{\partial \zeta_{\ell j}}{\partial u^k} + \frac{\partial \zeta_{k\ell}}{\partial u^j} - \frac{\partial \zeta_{jk}}{\partial u^\ell} \right). \quad (18)$$

In a small handful of systems [9, 28, 29], the friction tensor is analytically obtainable directly from the definition in (15). Zulkowski and DeWeese [30] derived an alternative form of the friction tensor in the special case of one-dimensional continuous over-damped dynamics, extending the range of analytically tractable models. Physically motivated approximations may also provide analytic insights when the full friction tensor is not known [16]. More often, numerical methods are required, typically involving estimation of the time-correlation functions using Markov-chain Monte Carlo simulations [12, 31, 32].

IV. FULL-CONTROL FRICTION TENSOR

Under the restriction of conservative driving, full control of a system refers to total control over the potential-energy landscape. Taking the $|\Omega\rangle$ state energies $V(s)$ as our control parameters, the conjugate forces are the random variables

$$\omega(s, t) = \delta(s - s(t)), \quad (19)$$

where $\delta(s - s(t))$ is the Kronecker delta function if the state space is discrete and the Dirac delta function if it is continuous. In the continuous case, the set of control parameters is uncountable, so we replace the partial derivative in (9) with a functional derivative:

$$\frac{\delta V(x)}{\delta V(y)} = \delta(x - y). \quad (20)$$

For discrete systems, $\omega_i(t)$ is an indicator function, returning one if the system is in state i at time t and zero

otherwise. For continuous systems, the integral of $\omega(x, t)$ over a finite region in Ω is an indicator function.

The average deviation of ω is precisely the deviation of the probability distribution from equilibrium:

$$\langle \delta\omega(s, t) \rangle \equiv \langle \delta\omega(s) \rangle_{p(t)} = \delta p(s, t), \quad (21)$$

for $\delta p(s, t) \equiv p(s, t) - \pi(s, V(t))$.

We define the full-control friction tensor as

$$\zeta(s, s'; V) \equiv \beta \int_0^\infty dt \langle \delta\omega(s, t) \delta\omega(s', 0) \rangle_{\pi(V)}. \quad (22)$$

As we shall see in the coming sections, $\zeta(V)$ has a non-empty null space spanned by $\mathbf{1}$ (the vector of all ones). This corresponds to the fact that uniformly raising or lowering the energy landscape has no effect on the system's dynamics. In terms of the geometry of the thermodynamic manifold, the full-control friction tensor $\zeta(V)$ is a degenerate metric ($\det \zeta(V) = 0$), and the full-control manifold \mathcal{M} is non-Riemannian.

In this section, we show that the properties of the full-control friction tensor (22) permit mathematical manipulations which significantly simplify the calculation of friction tensors. We briefly describe the Drazin inverse, a type of generalized inverse for singular square matrices which plays a central role in the derivations that follow. We then derive two decompositions of $\zeta(V)$ on discrete state spaces which we call the dynamical and spectral decompositions of the friction tensor. Next, we extend these results to continuous systems with countable spectra using an extension of the concept of the Drazin inverse to continuous linear operators.

A. Drazin Inverse of the Rate Matrix

The Drazin inverse of a matrix A is the unique matrix $A^{\mathcal{D}}$ such that [33]

$$A^{\nu_0} A^{\mathcal{D}} A = A^{\nu_0} \quad (23a)$$

$$A^{\mathcal{D}} A A^{\mathcal{D}} = A^{\mathcal{D}} \quad (23b)$$

$$A^{\mathcal{D}} A = A A^{\mathcal{D}}, \quad (23c)$$

where ν_0 is the index of the matrix A , i.e., the size of the largest Jordan block of A associated with the zero eigenvalue [34]. When $\nu_0 = 1$, such as for irreducible rate matrices [35], the Drazin inverse is a true generalized inverse since it satisfies $A A^{\mathcal{D}} A = A$, and is often called the group inverse [33]. In this case, the Drazin inverse may be constructed from

$$A^{\mathcal{D}} = P_0 + (A - P_0)^{-1}, \quad (24)$$

for projection matrix P_0 onto the null space $\mathcal{N}(A)$ of A .

From properties (23), one can show that [36]

$$A A^{\mathcal{D}} = I - P_0, \quad (25)$$

where I is the identity matrix. That is, $A A^{\mathcal{D}}$ projects vectors onto the complement of $\mathcal{N}(A)$. Thus, if \mathbb{W} is an irreducible rate matrix with equilibrium distribution π , the product $\mathbb{W} \mathbb{W}^{\mathcal{D}}$ maps a probability distribution to its deviation from equilibrium:

$$\mathbb{W} \mathbb{W}^{\mathcal{D}} \mathbf{p} = (I - \Pi) \mathbf{p} = \delta \mathbf{p}, \quad (26)$$

where $\Pi = \pi \otimes \mathbf{1} = [\pi \cdots \pi]$.

Additionally, (26) implies that $\mathbb{W} \mathbb{W}^{\mathcal{D}} \delta \mathbf{p} = \mathbb{W}^{\mathcal{D}} \mathbb{W} \delta \mathbf{p} = \delta \mathbf{p}$. Thus, under the restriction of the domain of \mathbb{W} and $\mathbb{W}^{\mathcal{D}}$ to vectors in the hyperplane $\{\mathbf{v} : \mathbf{1}^T \mathbf{v} = 0\}$, $\mathbb{W}^{\mathcal{D}}$ is a proper inverse of \mathbb{W} .

It follows from the commutativity of $\mathbb{W}^{\mathcal{D}}$ and \mathbb{W} that

$$\mathbb{W}^{\mathcal{D}} \pi = \mathbf{1} \mathbb{W}^{\mathcal{D}} = 0. \quad (27)$$

The Drazin inverse may be interpreted as ‘‘inverting the invertible part’’ of a matrix [36], leaving the null space of $\mathbb{W}^{\mathcal{D}}$ coincident with the null space of \mathbb{W} .

The Drazin inverse has appeared in previous works on optimal control [25, 36–38] and has applications in first-passage problems [39]. An alternative way to arrive at the Drazin inverse arises in the meromorphic functional calculus described in [34]. In Section IV C, we define and exploit an extension of the Drazin inverse to continuous linear operators.

B. Discrete State Space

1. Dynamical Decomposition

Since $\mathbb{W}^{\mathcal{D}}$ is a true inverse on the domain of probability deviations $\delta \mathbf{p}(t) = \langle \delta \boldsymbol{\omega}(t) \rangle$ (26),

$$\mathbb{W}^{\mathcal{D}} \mathbb{W} \langle \delta \boldsymbol{\omega}(t) \rangle = \mathbb{W}^{\mathcal{D}} \frac{d}{dt} \langle \delta \boldsymbol{\omega}(t) \rangle \quad (28a)$$

$$= \langle \delta \boldsymbol{\omega}(t) \rangle. \quad (28b)$$

By the law of total expectation, $\langle \delta \boldsymbol{\omega}(t) \otimes \delta \boldsymbol{\omega}(0) \rangle = \langle \langle \delta \boldsymbol{\omega}(t) | \delta \boldsymbol{\omega}(0) \rangle \otimes \delta \boldsymbol{\omega}(0) \rangle$, so that the full-control friction tensor (22) is

$$\zeta(\mathbf{V}) = \beta \mathbb{W}^{\mathcal{D}} \int_0^\infty dt \frac{d}{dt} \langle \delta \boldsymbol{\omega}(t) \delta \boldsymbol{\omega}(0) \rangle_{\pi(\mathbf{V})}. \quad (29)$$

Assuming a fixed energy landscape and ergodic dynamics, the correlations vanish in the infinite-time limit: $\lim_{t \rightarrow \infty} \langle \delta \boldsymbol{\omega}(t) \delta \boldsymbol{\omega}(0) \rangle = 0$. Thus

$$\zeta(\mathbf{V}) = -\beta \mathbb{W}^{\mathcal{D}} \Sigma_{\boldsymbol{\omega}}, \quad (30)$$

where $\Sigma_{\boldsymbol{\omega}} \equiv \langle \delta \boldsymbol{\omega} \otimes \delta \boldsymbol{\omega} \rangle_{\pi(\mathbf{V})}$ is the equilibrium covariance matrix of the conjugate force deviations.

In Appendix A we show that the equilibrium covariance matrix of the conjugate forces may be written as

$$\Sigma_{\boldsymbol{\omega}} = \text{diag} \{ \boldsymbol{\pi} \} - \boldsymbol{\pi} \otimes \boldsymbol{\pi}. \quad (31)$$

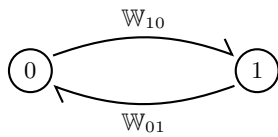


FIG. 1. General two-state system.

Since $\boldsymbol{\pi}$ is in the null space of $\mathbb{W}^{\mathcal{D}}$ (27), the decomposition (30) simplifies to

$$\zeta = -\beta \mathbb{W}^{\mathcal{D}} \text{diag} \{ \boldsymbol{\pi} \} . \quad (32)$$

This dynamical decomposition of the full-control friction tensor is our first major result. While obtaining the friction tensor from its definition (22) requires integration over a correlation function which is not typically known, the friction tensor in this form is obtained from the multiplication of matrices which are readily attained from the rate matrix \mathbb{W} . For small systems, this simplifies the analytic derivation of the friction tensor. For larger systems, this decomposition enables direct numerical calculation of friction tensors without recourse to simulations.

Example 1. Consider the general two-state Markov system in Fig. 1. The rates \mathbb{W}_{10} and \mathbb{W}_{01} are functions of $\mathbf{V} = [V^0, V^1]^T$. From the expression (24) for the Drazin inverse and the dynamical decomposition (32), the full-control friction tensor is

$$\zeta(\mathbf{V}) = \beta \frac{\mathbb{W}_{10} \mathbb{W}_{01}}{(\mathbb{W}_{10} + \mathbb{W}_{01})^3} \begin{bmatrix} 1 & -1 \\ -1 & 1 \end{bmatrix} . \quad (33)$$

As a concrete application, consider a single-level quantum dot interacting with a metallic reservoir [5]. In the wide-band approximation, the energy level ε of the quantum dot and the chemical potential μ of the reservoir set the respective tunnelling rates into and out of the reservoir as $\mathbb{W}_{10} = C[1 + e^{\beta(\mu - \varepsilon)}]^{-1}$ and $\mathbb{W}_{01} = C[1 + e^{\beta(\varepsilon - \mu)}]^{-1}$. The constant C sets the characteristic dynamical timescale. Then the friction tensor is

$$\zeta(\mathbf{V}) = \frac{1}{4C} \beta \text{sech}^2 \frac{1}{2} \beta(\varepsilon - \mu) \begin{bmatrix} 1 & -1 \\ -1 & 1 \end{bmatrix} . \quad (34)$$

The control parameters \mathbf{V} may be freely defined subject to the constraint

$$-\beta(V^1 - V^0) = \ln \frac{\pi_1}{\pi_0} . \quad (35)$$

For the quantum dot, it is natural to take either $V^0 = \mu$ and $V^1 = \varepsilon$ or $V^1 = \varepsilon - \mu$ with $V^0 = 0$ fixed. More generally, in the absence of physical motivations to the contrary, $V^i = -k_B T \ln \pi_i$ is a simple choice. All choices give the same friction tensor, since ζ is invariant under transformations $\mathbf{V} \mapsto \mathbf{V} + c\mathbf{1}$ for any $c \in \mathbb{R}$.

2. Comparing Decompositions

As noted in [9], the friction tensor ζ (for any set of control parameters) may be written as

$$\zeta = k_B T \mathcal{T} \circ \mathcal{I} , \quad (36)$$

the Hadamard product of the integral relaxation time matrix

$$\mathcal{T}_{ij} \equiv \int_0^\infty dt \frac{\langle \delta f_i(t) \delta f_j(0) \rangle_{\boldsymbol{\pi}}}{\langle \delta f_i \delta f_j \rangle_{\boldsymbol{\pi}}} \quad (37)$$

and the equilibrium Fisher information

$$\mathcal{I} \equiv \beta^2 \langle \delta \mathbf{f} \otimes \delta \mathbf{f} \rangle_{\boldsymbol{\pi}} = \beta^2 \Sigma_{\mathbf{f}} . \quad (38)$$

We compare this with the dynamical decomposition of the friction tensor,

$$\zeta = -k_B T \mathbb{W}^{\mathcal{D}} \mathcal{I} . \quad (39)$$

Defining the transition probability matrix with elements $p_{ij}(t) = \Pr [i, t | j, 0]$, the Drazin inverse is equivalently defined as [40]

$$-\mathbb{W}_{ij}^{\mathcal{D}} = \int_0^\infty dt [p_{ij}(t) - \pi_i] \quad (40a)$$

$$= \int_0^\infty dt \delta p_{ij}(t) . \quad (40b)$$

Thus, much like the integral relaxation time matrix \mathcal{T} , the Drazin inverse of the rate matrix describes the timescale of system relaxation. The magnitude of $\mathbb{W}_{ij}^{\mathcal{D}}$ characterizes how long it takes for $p_{ij}(t)$, the probability $p_i(t)$ conditioned on initialization in state j , to reach the equilibrium probability π_i .

When the conjugate forces \mathbf{f} are the indicator functions $\boldsymbol{\omega}$, equating (36) with the dynamical decomposition (32) gives

$$\mathbb{W}_{ij}^{\mathcal{D}} = \pi_i \mathcal{T}_{ij} , \quad i \neq j . \quad (41)$$

This relation offers an interpretation of the elements of the Drazin inverse of the rate matrix and provides a simple correspondence between the decomposition (36) and the dynamical decomposition (32) in the case of full control.

3. Spectral Decomposition

Using the notation from Section II, an irreducible rate matrix \mathbb{W} admits the spectral decomposition [35]

$$\mathbb{W} = - \sum_{\ell=1}^{|\Omega|-1} \lambda_\ell \boldsymbol{\psi}^{(\ell)} \otimes \boldsymbol{\phi}^{(\ell)} . \quad (42)$$

Each mode $\ell \neq 0$ has relaxation time

$$\tau_\ell \equiv \frac{1}{\lambda_\ell} . \quad (43)$$

We show in Appendix B that the Drazin inverse of \mathbb{W} decomposes similarly:

$$\mathbb{W}^{\mathcal{D}} = - \sum_{\ell=1}^{|\Omega|-1} \tau_{\ell} \psi^{(\ell)} \otimes \phi^{(\ell)}. \quad (44)$$

Under detailed balance, the right and left eigenvectors are related by $\phi^{(\ell)} = \text{diag}\{\pi\}^{-1} \psi^{(\ell)}$ [35]. Substituting (44) into the dynamical decomposition (32) yields the spectral decomposition of the friction tensor:

$$\zeta(\mathbf{V}) = \beta \sum_{\ell=1}^{|\Omega|-1} \tau_{\ell} \psi^{(\ell)} \otimes \psi^{(\ell)}. \quad (45)$$

This is our second major result. This form of the friction tensor demonstrates that modes with longer relaxation times contribute more to the friction tensor. The degeneracy of ζ is evident in this form: the orthonormality of the dual bases (5) implies that $\phi^{(0)} = \mathbf{1}$ is in the null-space of $\zeta(V)$.

In Section IV D 1 we show that this decomposition aids in the interpretation of optimal control strategies and in VI we apply it to uncover insights into the domain of applicability of the friction-tensor formalism.

Example 2. For the two-state system in Fig. 1,

$$\pi = \frac{1}{\mathbb{W}_{10} + \mathbb{W}_{01}} \begin{bmatrix} \mathbb{W}_{01} \\ \mathbb{W}_{10} \end{bmatrix}, \quad (46a)$$

$$\psi^{(1)} = \frac{\sqrt{\mathbb{W}_{01}\mathbb{W}_{10}}}{\mathbb{W}_{10} + \mathbb{W}_{01}} \begin{bmatrix} -1 \\ 1 \end{bmatrix}, \quad (46b)$$

where the prefactor of $\psi^{(1)}$ is obtained via the normalization condition

$$\langle \psi^{(1)}, \text{diag}\{\pi\}^{-1} \psi^{(1)} \rangle = 1. \quad (47)$$

The relaxation time is $\tau_1 = (\mathbb{W}_{10} + \mathbb{W}_{01})^{-1}$, and so the friction tensor is

$$\zeta(\mathbf{V}) = \beta \tau_1 \psi^{(1)} \otimes \psi^{(1)} \quad (48a)$$

$$= \beta \frac{\mathbb{W}_{01}\mathbb{W}_{10}}{(\mathbb{W}_{10} + \mathbb{W}_{01})^3} \begin{bmatrix} -1 \\ 1 \end{bmatrix} \begin{bmatrix} -1 & 1 \end{bmatrix}, \quad (48b)$$

consistent with Example 1.

C. Continuous State Space

We now consider a system on a continuous state space evolving according to the Fokker-Planck equation (2) with generator \mathcal{L} . When the Fokker-Planck operator has a countable spectrum, it admits the spectral decomposition [41]

$$\mathcal{L}(x, y) = - \sum_{\ell=1}^{\infty} \lambda_{\ell} \psi^{(\ell)}(x) \phi^{(\ell)}(y). \quad (49)$$

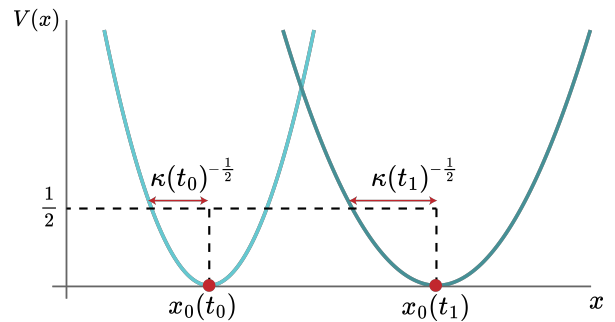


FIG. 2. Harmonic trap $V(x, t) = \frac{1}{2}\kappa(t)(x - x_0(t))^2$ with tunable stiffness κ and trap center x_0 considered in Example 3.

In Appendix C, we show that the operator defined by

$$\mathcal{L}^{\mathcal{D}}(x, y) = - \sum_{\ell=1}^{\infty} \tau_{\ell} \psi^{(\ell)}(x) \phi^{(\ell)}(y) \quad (50)$$

satisfies continuous analogs of the properties (23) and (26) of the Drazin inverse of a matrix. Then

$$\zeta(x, y; V) = \beta \int_0^{\infty} dt \langle \delta\omega(x, t) \delta\omega(y, 0) \rangle \quad (51a)$$

$$= \beta \int_{\Omega} dz \mathcal{L}^{\mathcal{D}}(x, z) \int_0^{\infty} dt \frac{d}{dt} \langle \delta\omega(x, t) \delta\omega(y, 0) \rangle. \quad (51b)$$

The dynamical decomposition of the full-control friction tensor for a continuous system is thus

$$\zeta(x, y; V) = -\beta \int_{\Omega} dz \mathcal{L}^{\mathcal{D}}(x, z) \Sigma_{\omega}(z, y). \quad (52)$$

Using $\Sigma_{\omega}(x, y) = \pi(x)\delta(x - y) - \pi(x)\pi(y)$ (see Appendix A) and the orthonormality of the eigenfunctions (5), the dynamical decomposition simplifies to

$$\zeta(x, y; V) = -\beta \mathcal{L}^{\mathcal{D}}(x, y) \pi(y). \quad (53)$$

Substituting (50) gives the spectral decomposition

$$\zeta(x, y; V) = \beta \sum_{\ell=1}^{\infty} \tau_{\ell} \psi^{(\ell)}(x) \psi^{(\ell)}(y). \quad (54)$$

Example 3. Consider a particle diffusing in a one-dimensional harmonic trap with stiffness constant κ and trap center x_0 , and hence potential energy $V(x) = \frac{1}{2}\kappa(x - x_0)^2$ (Fig. 2). The Fokker-Planck operator is

$$\mathcal{L} \cdot = \frac{\partial}{\partial x} \left[D \exp \left\{ -\frac{V(x)}{D} \right\} \frac{\partial}{\partial x} \left(\exp \left\{ \frac{V(x)}{D} \right\} \right) \right], \quad (55)$$

for diffusion constant D . The eigenfunctions of \mathcal{L}

are [42]

$$\psi^{(\ell)}(x) = \sqrt{\frac{\kappa}{2\pi D}} \frac{(-1)^\ell}{\ell!} \left(\frac{D}{\kappa}\right)^{\frac{\ell}{2}} \frac{d^\ell}{dx^\ell} \exp\left\{-\frac{V(x)}{D}\right\}, \quad (56)$$

and the corresponding relaxation times are

$$\tau_\ell = \frac{1}{\ell\kappa}. \quad (57)$$

Substituting the eigenfunctions and relaxation times into the spectral decomposition (54) gives the friction tensor. Note that the expression for $V(x)$ has only two controllable parameters: κ and x_0 . It is thus unnecessary to consider every element of the full-control friction tensor. In Section V, we demonstrate how to build a parametric-control friction tensor from the full-control friction tensor.

D. Discussion

1. Spectral Decomposition of the Excess Power

The spectral decompositions for discrete systems (45) and continuous systems (54) yield a decomposition of the linear-response excess power (11):

$$\langle \mathcal{P}_{\text{ex}}(t) \rangle^{\text{LR}} = \sum_{j \geq 1} \tau_j \left\langle \frac{dV}{dt}, \psi^{(j)} \right\rangle^2. \quad (58)$$

This shows that the linear-response excess power can be separated into a sum of independent contributions associated with the fixed-parameter modes of the underlying system, providing insight into the dynamical origin of dissipation. Roughly, each term captures the degree to which the protocol traverses a given mode, scaled by that mode's relaxation time. This provides a design principle for minimum-work protocols: dissipation may be reduced by driving a system such that dV/dt is maximally orthogonal to modes with long relaxation times.

2. Geodesics and Generalized Christoffel Symbols

Let Ω be finite. Since $\zeta(\mathbf{V})$ is a degenerate metric, it is not invertible, and the Christoffel symbols of the second kind (18) do not exist. Thus, we cannot immediately apply the geodesic equations (17) to find the minimum work protocols; however, the Christoffel symbols can be generalized using the Drazin inverse of the friction tensor to obtain geodesic equations.

A minimum-work protocol $\mathbf{V}(t)$ satisfies

$$-\frac{1}{2} \frac{\delta \langle \mathcal{W}_{\text{ex}} \rangle^{\text{LR}}}{\delta V^k(t)} = \sum_j \zeta_{kj} \frac{d^2 V^j}{dt^2} + \sum_{ij} \Gamma_{kij} \frac{dV^i}{dt} \frac{dV^j}{dt} = 0, \quad (59)$$

for Christoffel symbols of the first kind

$$\Gamma_{ijk} \equiv \frac{1}{2} \left(\frac{\partial \zeta_{ij}}{\partial V^k} + \frac{\partial \zeta_{ki}}{\partial V^j} - \frac{\partial \zeta_{jk}}{\partial V^i} \right). \quad (60)$$

Since the null space of $\zeta(\mathbf{V})$ is spanned by the vector $\mathbf{1}$,

$$\zeta^{\mathcal{D}} \zeta \frac{d\mathbf{V}}{dt} = \frac{d\mathbf{V}}{dt} - c\mathbf{1}, \quad (61)$$

where $c \in \mathbb{R}$. Defining the generalized Christoffel symbols of the second kind as

$$\Gamma_{jk}^i \equiv \sum_\ell (\zeta^{\mathcal{D}})^{i\ell} \Gamma_{\ell jk}, \quad (62)$$

solving the geodesic equation (17) gives MWPs.

Example 4. Consider again the two-state system from Fig. 1. The Drazin inverse of the friction tensor is

$$\zeta^{\mathcal{D}} = \frac{(\mathbb{W}_{01} + \mathbb{W}_{10})^3}{4\mathbb{W}_{01}\mathbb{W}_{10}} \begin{bmatrix} 1 & -1 \\ -1 & 1 \end{bmatrix}. \quad (63)$$

For a two-state system, the detailed-balance condition dictates that \mathbb{W}_{10} and \mathbb{W}_{01} depend only on the energy difference $\Delta \equiv V^0 - V^1$. Applying the definition of the generalized Christoffel symbols of the second kind,

$$\Gamma_{jk}^i = \frac{1}{4} (-1)^{i+j+k} \frac{\partial \ln \xi}{\partial \Delta}, \quad (64)$$

for $\xi(\Delta) \equiv \mathbb{W}_{01}\mathbb{W}_{10}/(\mathbb{W}_{01} + \mathbb{W}_{10})^3$. The geodesic equations (17) reduce to a single differential equation in Δ :

$$\ddot{\Delta}(t) + \frac{1}{2} \frac{\partial \ln \xi}{\partial \Delta} \dot{\Delta}^2(t) = 0. \quad (65)$$

For the example of the single-level quantum dot where $\Delta = \epsilon - \mu$,

$$\frac{\partial \ln \xi}{\partial \Delta} = -\beta \tanh \frac{\beta \Delta}{2}. \quad (66)$$

V. PARAMETRIC CONTROL

In typical settings, the number of control parameters is significantly smaller than the number of system states. For instance, early studies of fluctuation theorems involved the manipulation of single RNA molecules with the total extension of the strand as the only controllable

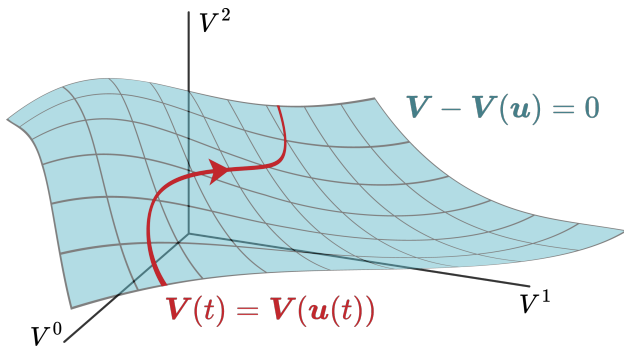


FIG. 3. A parameterization of the potential V by control-parameter vector $\mathbf{u} \in \mathbb{R}^m$ with $m < |\Omega|$ (typically $m \ll |\Omega|$) constitutes a restriction of protocols to a hypersurface within the full-control space. The $m \times m$ metric tensor $\zeta(\mathbf{u})$ is a metric on this submanifold inherited from the full-control friction tensor $\zeta(V)$.

parameter [43, 44]. The success of these demonstrations and other nonequilibrium measurements of equilibrium free-energy landscapes relies on executing experimental protocols with low excess work [45]. Partial (or parametric) control is thus an area of clear practical importance.

Let $\mathbf{u} \in \mathbb{R}^m$ be the vector of control parameters. Under the assumption of conservative driving, a control protocol $\mathbf{u}(t)$ results in a time-dependent potential $V(t) = V(\mathbf{u}(t))$. Figure 3 illustrates that this involves the restriction of control protocols to a hypersurface of constraint defined by

$$V - V(\mathbf{u}) = 0. \quad (67)$$

The corresponding friction tensor $\tilde{\zeta}(\mathbf{u})$ is the metric on this submanifold inherited from the full-control friction tensor $\zeta(V)$. In a slight abuse of notation, we will drop the tilde from $\zeta(\mathbf{u})$ and instead specify the appropriate control manifold by explicitly writing the argument of ζ when necessary.

A. General Sets of Control Parameters

1. Discrete Systems

Define the Jacobian matrix $\mathbb{J} \in \mathbb{R}^{n \times m}$ of the parameterization of V as

$$\mathbb{J}_{ij} = \frac{\partial V^i}{\partial u^j}. \quad (68)$$

The inherited metric on the hypersurface (67) is

$$\zeta(\mathbf{u}) = \mathbb{J}^T \zeta(\mathbf{V}(\mathbf{u})) \mathbb{J}. \quad (69)$$

The control-parameter velocities transform as

$$\mathbb{J} \frac{d\mathbf{u}}{dt} = \frac{d\mathbf{V}}{dt}, \quad (70)$$

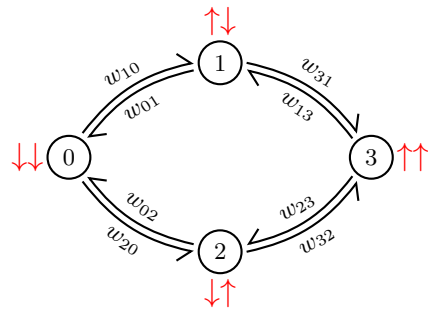


FIG. 4. Markov-state diagram for two-spin system.

confirming that the excess power is invariant under this transformation:

$$\frac{d\mathbf{u}^T}{dt} \zeta(\mathbf{u}) \frac{d\mathbf{u}}{dt} = \frac{d\mathbf{V}^T}{dt} \zeta(\mathbf{V}(\mathbf{u})) \frac{d\mathbf{V}}{dt}. \quad (71)$$

The Jacobian matrix (68) is closely related to the conjugate forces to \mathbf{u} , with $\mathbb{J}_{ij} = -f_j(s_i)$, where $f_j(s_i)$ is the value of the j th conjugate force when the system is in state i . Thus

$$\mathbb{J}^T \langle \boldsymbol{\omega}(t) \rangle = \mathbb{J}^T \mathbf{p}(t) \quad (72a)$$

$$= \langle \mathbf{f}(t) \rangle. \quad (72b)$$

In the language of differential geometry, the transformation laws (70) and (72) express the duality of the control parameters and conjugate forces: the control parameters transform contravariantly, while the conjugate forces transform covariantly [26].

Define the conjugate relaxation modes by

$$\tilde{\boldsymbol{\psi}}^{(k)} = \mathbb{J}^T \boldsymbol{\psi}^{(k)}. \quad (73)$$

For the zeroth mode, $\tilde{\boldsymbol{\psi}}^{(0)} = -\langle \mathbf{f} \rangle_{\pi}$. In light of (72), $\tilde{\boldsymbol{\psi}}^{(k)}$ for $k = 1, 2, \dots$ captures the fixed-parameter relaxation of $\langle \mathbf{f}(t) \rangle$ associated with the k th mode of the system with relaxation time τ_k . We show in Section VB that for some sets of control parameters $\mathbf{u} \in \mathbb{R}^m$ with $m = |\Omega| - 1$, the probability distribution is related to the average of conjugate forces by an invertible affine transformation which we construct from \mathbb{J} by generalizing the Drazin inverse to rectangular matrices.

For any set of control parameters, the excess power can be expressed as a sum of contributions from the respective conjugate modes: from the transformation law (70) and the definition (73), it follows that $\langle d\mathbf{V}/dt, \boldsymbol{\psi}^{(\ell)} \rangle = \langle d\mathbf{u}/dt, \tilde{\boldsymbol{\psi}}^{(\ell)} \rangle$. The spectral decomposition of the linear-response excess power (58) thus becomes

$$\langle \mathcal{P}_{\text{ex}}(t) \rangle^{\text{LR}} = \sum_{i=1}^{|\Omega|-1} \tau_i \left\langle \frac{d\mathbf{u}}{dt}, \tilde{\boldsymbol{\psi}}^{(i)} \right\rangle^2. \quad (74)$$

Example 5. Consider a two-spin system (σ_0, σ_1) , $\sigma_i = \pm 1$, with spin-spin coupling strength J and independent external fields h_0 and h_1 . The potential energy is

$$V = -J\sigma_0\sigma_1 - h_0\sigma_0 - h_1\sigma_1. \quad (75)$$

For single-spin-flip dynamics, one choice of transition rates from state j to state i is

$$\mathbb{W}_{ij} = \frac{1}{1 + e^{\beta(V^i - V^j)}}. \quad (76)$$

The Markov-state diagram in Fig. 4 shows a canonical ordering of states.

Though laborious to solve by hand, an analytic form for the full-control friction tensor is obtained from the dynamical decomposition (32) using symbolic software such as *Maple* [46]. We may consider a variety of submanifolds. For instance, the friction tensor for independent control over the coupling J and the fields h_0 and h_1 is obtained via the transformation law (69) with the Jacobian

$$\mathbb{J} = \begin{bmatrix} -1 & -1 & 1 \\ 1 & -1 & -1 \\ -1 & 1 & -1 \\ 1 & 1 & 1 \end{bmatrix} \begin{matrix} s_0 \\ s_1 \\ s_2 \\ s_3 \end{matrix}. \quad (77)$$

$\sigma_0 \quad \sigma_1 \quad \sigma_0\sigma_1$

By contrast, for fixed coupling J and one-parameter control over a global field $h_0 = h_1 \equiv h$, the Jacobian is

$$\mathbb{J} = \begin{bmatrix} -2 \\ 0 \\ 0 \\ 2 \end{bmatrix} \begin{matrix} s_0 \\ s_1 \\ s_2 \\ s_3 \end{matrix}, \quad (78)$$

$\sigma_0 + \sigma_1$

giving friction tensor (here a friction coefficient)

$$\zeta(h) = 4(\zeta_{00} - 2\zeta_{03} + \zeta_{33}). \quad (79)$$

The absence of terms involving the anti-aligned states 1 and 2 in $\zeta(h)$ reflects the fact that the energies of these states are unaffected by the value of the global magnetic field h .

2. Continuous Systems

The analysis is nearly identical for continuous systems with discrete spectra. Given parametric control over a continuous potential V , the protocol velocity may be ex-

pressed as

$$\frac{dV}{dt} = \sum_{i=1}^m \frac{du^i}{dt} \frac{\partial V(x, t)}{\partial u^i}. \quad (80)$$

This defines a ‘‘Jacobian’’ with one continuous index x and one discrete index i :

$$\mathbb{J}_{x,i} \equiv \frac{\partial V(x)}{\partial u^i}. \quad (81)$$

Invariance of the excess power is guaranteed for the transformation law

$$\zeta_{ij} = \int_{\Omega \times \Omega} dx dy \mathbb{J}_{x,i} \zeta(x, y) \mathbb{J}_{y,j}. \quad (82)$$

Defining the conjugate modes to be the \mathbb{R}^m vectors

$$\tilde{\psi}^{(i)} = \int_{\Omega} dx \nabla_{\mathbf{u}} V(x) \psi^{(i)}(x), \quad (83)$$

the friction tensor becomes

$$\zeta(\mathbf{u}) = \sum_{i=1}^{\infty} \tau_i \tilde{\psi}^{(i)} \otimes \tilde{\psi}^{(i)}. \quad (84)$$

The spectral decomposition of the excess power is obtained by replacing $|\Omega| - 1$ with ∞ in the discrete-system result (74).

Example 6. Consider again the harmonic trapping potential from Example 3. For the two control parameters $\mathbf{u} = [x_0, \kappa]^T$, the conjugate forces are

$$f_{x_0}(x) = -\kappa(x - x_0) \quad (85a)$$

$$= -\sqrt{\kappa D} \phi^{(1)}(x), \quad (85b)$$

$$f_{\kappa}(x) = -\frac{1}{2}(x - x_0)^2 \quad (85c)$$

$$= -\frac{D}{2\kappa} [\phi^{(0)}(x) + \phi^{(2)}(x)]. \quad (85d)$$

From (85b) and (85d), the linear response to changes of the trap center and strength involves only the first two modes. From the eigenfunctions (56) and relaxation times (57), the decomposition of the friction tensor is thus

$$\zeta(\mathbf{u}) = \tau_1 \begin{bmatrix} \kappa D & 0 \\ 0 & 0 \end{bmatrix} + \tau_2 \begin{bmatrix} 0 & 0 \\ 0 & \frac{D^2}{4\kappa^2} \end{bmatrix} \quad (86a)$$

$$= \begin{bmatrix} D & 0 \\ 0 & \frac{D^2}{8\kappa^3} \end{bmatrix}. \quad (86b)$$

B. Complete Set of Control Parameters

Since $\mathbf{1}$ is in the null space of $\zeta(V)$, the full-control friction tensor is degenerate. This corresponds physically to

the invariance of the dynamics under global raising and lowering of the potential-energy landscape. This formulation is thus over-determined: for a discrete system with $|\Omega| = n$ states, full control is possible with a set of $n - 1$ control parameters.

We call the control-parameter vector $\mathbf{u} \in \mathbb{R}^{n-1}$ “complete” if there exists a generalized inversion of the parameterization $\mathbf{V}(\mathbf{u})$ such that

$$\mathbf{u}(\mathbf{V}) = \mathbf{u}(\mathbf{V}') \iff \mathbf{V}' = \mathbf{V} + c\mathbf{1} \quad (87)$$

for some $c \in \mathbb{R}$. In other words, the control parameters \mathbf{u} completely determine the potential energy \mathbf{V} up to a global additive constant.

Let $\mathbb{J} \in \mathbb{R}^{n \times (n-1)}$ be the Jacobian for a complete set of control parameters. The condition (87) implies that $\text{rank } \mathbb{J} = n - 1$ and that $\mathcal{N}(\mathbb{J}^T) = \text{span}\{\mathbf{1}\}$. Then \mathbb{J} has a left inverse $\mathbb{J}^L = (\mathbb{J}^T \mathbb{J})^{-1} \mathbb{J}^T$ such that

$$\mathbb{J}^L \mathbb{J} = I_{(n-1) \times (n-1)} \quad (88)$$

where $I_{k \times k}$ denotes the identity matrix on \mathbb{R}^k .

Since $\mathbb{J} \mathbb{J}^T$ is not invertible, the right inverse $\mathbb{J}^R = \mathbb{J}^T (\mathbb{J}^T \mathbb{J})^{-1}$ of the Jacobian does not exist, but a generalization of the Drazin inverse to rectangular matrices is

$$\mathbb{J}^{\mathcal{D}R} \equiv \mathbb{J}^T (\mathbb{J} \mathbb{J}^T)^{\mathcal{D}} . \quad (89)$$

Since $\mathcal{N}(\mathbb{J} \mathbb{J}^T) = \mathcal{N}(\mathbb{J}^T)$ [47], the properties of the Drazin inverse (Section IV A) impose

$$\mathbb{J} \mathbb{J}^{\mathcal{D}R} = I_{n \times n} - \frac{1}{n} \mathbb{1}_{n \times n} , \quad (90)$$

where $\mathbb{1}_{n \times n}$ is the $n \times n$ matrix of ones.

Multiplying both sides of the conjugate-force transformation law (72) by the right Drazin inverse shows that for a complete set of control parameters, the probability distribution is uniquely determined from the conjugate-force average by the affine transformation

$$\mathbf{p}(t) = (\mathbb{J}^{\mathcal{D}R})^T \langle \mathbf{f}(t) \rangle + \frac{1}{n} \mathbf{1} . \quad (91)$$

For a complete set of control parameters, the time evolution of the average conjugate-force deviation $\langle \delta \mathbf{f}(t) \rangle$ is self-contained in the sense that

$$\frac{d \langle \delta \mathbf{f}(t) \rangle}{dt} = \mathbb{W}_{\mathbf{f}} \langle \delta \mathbf{f}(t) \rangle , \quad (92)$$

where

$$\mathbb{W}_{\mathbf{f}} \equiv \mathbb{J}^T \mathbb{W} (\mathbb{J}^{\mathcal{D}R})^T \quad (93)$$

is the generator of the dynamics of $\langle \mathbf{f}(t) \rangle$.

Using the definition (89) and the fact that $\mathbf{1}$ is a null left-eigenvector of $\mathbb{W}^{\mathcal{D}}$, it is straightforward to verify that

$$\mathbb{W}_{\mathbf{f}}^{-1} = \mathbb{J}^T \mathbb{W}^{\mathcal{D}} (\mathbb{J}^{\mathcal{D}R})^T . \quad (94)$$

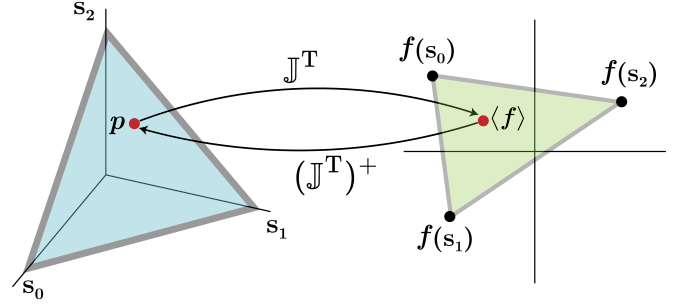


FIG. 5. When the space Δ_f of conjugate-force averages $\langle \mathbf{f} \rangle$ forms an $(n-1)$ -simplex in \mathbb{R}^{n-1} (green triangle), there exists an inverse affine transformation $(\mathbb{J}^T)^+$ from the conjugate-force average to the distribution \mathbf{p} , which is constrained to the standard $(n-1)$ -simplex in \mathbb{R}^n (blue triangle).

Further, from $\mathbb{J}_{ij} = -f_j(s_i)$,

$$\mathbb{J}^T \text{diag}\{\boldsymbol{\pi}\} \mathbb{J} = \langle \mathbf{f} \otimes \mathbf{f} \rangle_{\boldsymbol{\pi}} . \quad (95)$$

Thus the friction tensor for a complete set of control parameters \mathbf{u} has the dynamical decomposition

$$\zeta(\mathbf{u}) = -\mathbb{W}_{\mathbf{f}}^{-1} \langle \mathbf{f} \otimes \mathbf{f} \rangle_{\boldsymbol{\pi}} . \quad (96)$$

There is an intuitive geometric statement which is equivalent to the completeness condition (87). An $(n-1)$ -dimensional simplex is an $(n-1)$ -dimensional polytope with n vertices—this generalizes the definition of a triangle (a 2-dimensional polytope with 3 vertices) to arbitrary dimensions [48]. The set of probability vectors \mathbf{p} defines the probability simplex $\Delta^{(n-1)} = \{\mathbf{p} \in \mathbb{R}^n : \mathbf{1}^T \mathbf{p} = 1\}$. Let Δ_f be the convex hull of the n points $\{\mathbf{f}(s_i)\}$, i.e., the set of all conjugate-force averages $\langle \mathbf{f} \rangle$. For a complete set of control parameters, Δ_f is an $(n-1)$ -dimensional simplex in \mathbb{R}^{n-1} and \mathbb{J}^T is an invertible map from $\Delta^{(n-1)}$ to Δ_f . Put simply, the space of conjugate-force averages $\langle \mathbf{f} \rangle$ for a complete set of control parameters is the same “size” as the space of probability vectors. Figure 5 illustrates this for a three-state system.

VI. ACCURACY AND HIGHER-ORDER CORRECTIONS

In this section, we apply the spectral decomposition (45) to analyze the accuracy of the linear-response approximation. This analysis provides an explanation of the high accuracy of the approximation for MWPs beyond the naive domain of applicability, offering insight into what it means for a protocol to be sufficiently “slow”. We provide higher-order corrections to the friction tensor, following an approach introduced in [25]. Throughout this section we assume a discrete state space, though analysis is similar for continuous systems with discrete spectra.

A. Domain of Applicability

Properties (26) and (27) of the Drazin inverse allow us to write the deviation of the probability distribution $\mathbf{p}(t)$ from the equilibrium $\boldsymbol{\pi}(t) = \boldsymbol{\pi}(\mathbf{V}(t))$ as

$$\delta\mathbf{p}(t) = \mathbb{W}^{\mathcal{D}} \frac{d\delta\mathbf{p}(t)}{dt} + \mathbb{W}^{\mathcal{D}} \frac{d\boldsymbol{\pi}}{dt}, \quad (97)$$

as seen in Eq. (12) of [25]. The time derivative $\frac{d}{dt}$ is a total derivative accounting both for the relaxation of the distribution under \mathbb{W} for fixed potential V and the evolution of the equilibrium distribution $\boldsymbol{\pi}$ under the protocol $\mathbf{V}(t)$.

Writing the time derivative of $\boldsymbol{\pi}$ in terms of the protocol velocity,

$$\frac{d\pi_k}{dt} = \sum_j \frac{dV^j}{dt} \frac{\partial \pi_k}{\partial V^j} \quad (98a)$$

$$= -\beta\pi_k \sum_j \frac{dV^j}{dt} (\delta_{jk} - \pi_j), \quad (98b)$$

and applying the dynamical decomposition (32) gives

$$\mathbb{W}^{\mathcal{D}} \frac{d\boldsymbol{\pi}}{dt} = \zeta \frac{d\mathbf{V}}{dt}. \quad (99)$$

Combining (97) and (99) and applying the spectral decomposition (44) of the Drazin inverse of the rate matrix to the error $\epsilon(t)$ of the linear-response approximation for the excess power,

$$\epsilon(t) \equiv \langle \mathcal{P}_{\text{ex}}(t) \rangle - \langle \mathcal{P}_{\text{ex}}(t) \rangle^{\text{LR}} \quad (100a)$$

$$= \frac{d\mathbf{V}^{\text{T}}}{dt} \delta\mathbf{p}(t) - \langle \mathcal{P}_{\text{ex}}(t) \rangle^{\text{LR}}, \quad (100b)$$

yields

$$\epsilon(t) = - \sum_{i=1}^{|\Omega|-1} \tau_i \left\langle \frac{d\mathbf{V}}{dt}, \boldsymbol{\psi}^{(i)} \right\rangle \left\langle \boldsymbol{\phi}^{(i)}, \frac{d\delta\mathbf{p}}{dt} \right\rangle. \quad (101)$$

If we assume that the system remains near equilibrium throughout the protocol, then $\frac{d\delta\mathbf{p}}{dt}$ —and hence the term $\left\langle \boldsymbol{\phi}^{(i)}, \frac{d\delta\mathbf{p}}{dt} \right\rangle$ in the error—remains small throughout the protocol, ensuring that the linear-response approximation is accurate.

The factor $\tau_i \left\langle \frac{d\mathbf{V}}{dt}, \boldsymbol{\psi}^{(i)} \right\rangle$ appears in both the error (101) and the excess power (58). The linear-response approximation is thus self-reinforcing in the sense that a protocol that reduces the linear-response excess work simultaneously reduces the error. This agrees with the observation in [20] that the LR approximation performs remarkably well beyond the naively defined domain of applicability.

In summary, (101) clarifies the meaning of “slow” driving in this context. Driving that is slow relative to *all* relaxation timescales produces small-magnitude $d(\delta\mathbf{p})/dt$ since the system remains close to equilibrium throughout

the protocol. This is a sufficient condition for the accuracy of the linear-response approximation, but it is not strictly necessary—due to the multi-exponential relaxation, the friction-tensor formalism can apply even if the magnitude of $d\mathbf{V}/dt$ is large with respect to the longest relaxation timescale, as long as this velocity is mostly parallel to fast modes (or, equivalently, mostly orthogonal to slow modes).

B. Series Expansion of Excess Power

From Section VI A, the excess power can be separated into a linear-response term and a term capturing all higher-order contributions:

$$\langle \mathcal{P}_{\text{ex}}(t) \rangle = \langle \mathcal{P}_{\text{ex}}(t) \rangle^{\text{LR}} + \frac{d\mathbf{V}^{\text{T}}}{dt} \mathbb{W}^{\mathcal{D}} \frac{d\delta\mathbf{p}}{dt}. \quad (102)$$

Following [25], iterative substitution of (97) into (102) gives the excess power as the infinite series

$$\langle \mathcal{P}_{\text{ex}}(t) \rangle = \sum_{i=1}^{\infty} \langle \mathcal{P}_{\text{ex}}(t) \rangle^{(n)}, \quad (103)$$

where

$$\langle \mathcal{P}_{\text{ex}}(t) \rangle^{(n)} = \frac{d\mathbf{V}^{\text{T}}}{dt} \left[\left(\mathbb{W}^{\mathcal{D}} \frac{d}{dt} \right)^{n-1} \zeta(\mathbf{V}) \right] \frac{d\mathbf{V}}{dt}. \quad (104)$$

The linear-response excess power corresponds to $n = 1$. Additional analysis would be necessary to understand the convergence properties of (103). Consider, for instance, the first correction term

$$\langle \mathcal{P}_{\text{ex}}(t) \rangle^{(2)} = \sum_{ijk} \frac{dV^i}{dt} \frac{dV^j}{dt} \frac{dV^k}{dt} \zeta_{ijk}^{(2)}, \quad (105)$$

where

$$\zeta_{ijk}^{(2)} \equiv \sum_{\ell} \mathbb{W}^{\mathcal{D}}_{i\ell} \frac{\partial \zeta_{\ell k}}{\partial V^j} \quad (106a)$$

$$= - \sum_{\ell} \frac{\zeta_{i\ell}}{\pi_{\ell}} \frac{\partial \zeta_{\ell k}}{\partial V^j}. \quad (106b)$$

The correction term (105) is not strictly positive, and without additional insight into the convergence properties of the series (103) it is not immediately clear whether and to what extent this added term improves on the linear-response approximation. Furthermore, for $n > 3$ the n th term in the series involves the derivative $d^{n-1}\mathbf{V}/dt^{n-1}$, so that solution of the Euler-Lagrange equation for the MWP becomes significantly more complex as higher-order terms are added.

VII. SUMMARY AND OUTLOOK

We have presented a reformulation of the friction-tensor formalism for conservative control of stochastic

systems. A global thermodynamic manifold \mathcal{M} is defined, with a metric structure provided by the full-control friction tensor from which all parametric-control friction tensors may be derived as inherited metrics on submanifolds of \mathcal{M} . This framework was derived for both discrete state spaces and continuous state spaces for which the Fokker-Planck operator \mathcal{L} has a discrete spectrum.

Exploiting the properties of a type of generalized inverse called the Drazin inverse, we derived dynamical and spectral decompositions of the full-control friction tensor. From this analysis, we showed that the linear-response contribution to the excess power may be decomposed into a sum of terms respectively corresponding to each of the system's relaxation modes (58). The magnitude of the k th term depends on the degree to which the protocol traverses that mode, scaled by its relaxation time τ_k . This decomposition suggests a design principle for protocols that reduce excess dissipation for finite-time processes: drive a system such that dV/dt is maximally orthogonal to modes with long relaxation times, subject to the constraints set by the protocol endpoints, and for parametric control the parameterization $V(\mathbf{u})$.

Application of the spectral decomposition to the approximation accuracy sheds light on the observation that the friction-tensor formalism performs well far beyond its naive domain of applicability [20]: the formalism is self-reinforcing in the sense that minimization of the approximate excess work simultaneously reduces the magnitude of the approximation error.

For discrete systems with small state spaces or for systems whose spectra are known analytically, these decompositions simplify the analytic calculation of the friction tensor. For larger systems, the dynamical decomposition (32) enables numerical calculation of the friction tensor without recourse to numerical simulations, with the matrix inversion in (24) acting as the computational bottleneck; however, for very large discrete systems or fine discretizations of continuous systems, this approach becomes prohibitively expensive. When a large spectral gap exists (i.e., $\tau_1 \geq \dots \tau_q \gg \tau_{q+1} \geq \dots$ for some q), truncation of the spectral decomposition (45) may enable controlled-accuracy approximation of the friction tensor.

ACKNOWLEDGMENTS

This work was supported by a Natural Sciences and Engineering Research Council of Canada (NSERC) Undergraduate Student Research Award (J.R.S.), an NSERC CGS Master's scholarship (J.R.S.), an NSERC Discovery Grant RGPIN-2020-04950 (D.A.S.), and a Tier-II Canada Research Chair CRC-2020-00098 (D.A.S.).

Appendix A: Equilibrium Covariance Matrix

In Section IV B 1 we obtain an expression for the full-control friction tensor (30) involving the equilibrium covariance matrix $\Sigma_\omega \equiv \langle \delta\omega \otimes \delta\omega \rangle$ of the conjugate forces $\delta\omega$ (19). The random variable $\omega_i(t)$ is an indicator function, returning one if the system is in state i at time t and zero otherwise. It follows that $\langle \omega \rangle_{\mathbf{p}} = \mathbf{p}$. Then the ij component of Σ_ω is

$$(\Sigma_\omega)_{ij} = \langle \delta\omega_i \delta\omega_j \rangle \quad (\text{A1a})$$

$$= \langle \omega_i \omega_j \rangle - \langle \omega_i \rangle \langle \omega_j \rangle \quad (\text{A1b})$$

$$= \sum_k \pi_k \delta_{ik} \delta_{jk} - \pi_i \pi_j \quad (\text{A1c})$$

$$= \pi_i \delta_{ij} - \pi_i \pi_j, \quad (\text{A1d})$$

or in matrix form,

$$\Sigma_\omega = \text{diag}\{\boldsymbol{\pi}\} - \boldsymbol{\pi} \otimes \boldsymbol{\pi}. \quad (\text{A2})$$

For continuous systems, the conjugate forces have continuous indices and the corresponding equilibrium covariances are defined as $\Sigma_\omega(x, y) = \langle \delta\omega(x) \delta\omega(y) \rangle$. We obtain an analogous expression to (A2):

$$\begin{aligned} \langle \delta\omega(x) \delta\omega(y) \rangle &= \int_\Omega dz \pi(z) \delta(y-z) \delta(x-z) - \pi(x) \pi(y) \quad (\text{A3a}) \\ &= \pi(x) \delta(x-y) - \pi(x) \pi(y). \quad (\text{A3b}) \end{aligned}$$

Appendix B: Spectral Decomposition of the Drazin Inverse of \mathbb{W}

We derive the spectral decomposition (44) of the Drazin inverse $\mathbb{W}^{\mathcal{D}}$ of an irreducible rate matrix \mathbb{W} . The irreducibility of \mathbb{W} implies that it has index $\nu_0 = 1$, and the Drazin inverse may be constructed from

$$\mathbb{W}^{\mathcal{D}} = \Pi + (\mathbb{W} - \Pi)^{-1}, \quad (\text{B1})$$

where $\Pi = [\boldsymbol{\pi} \dots \boldsymbol{\pi}] = \boldsymbol{\psi}^{(0)} \otimes \boldsymbol{\phi}^{(0)}$ is the projection onto the null space of \mathbb{W} .

Let $\boldsymbol{\psi}^{(\ell)}$ be a right eigenvector of \mathbb{W} with eigenvalue $-\lambda_\ell$. Then

$$(\mathbb{W} - \Pi) \boldsymbol{\psi}^{(\ell)} = -(\lambda_\ell + \delta_{0\ell}) \boldsymbol{\psi}^{(\ell)} \quad (\text{B2a})$$

$$= -\lambda'_\ell \boldsymbol{\psi}^{(\ell)}. \quad (\text{B2b})$$

Thus $\mathbb{W} - \Pi$ has the same eigenvectors as \mathbb{W} and has strictly non-zero eigenvalues $-\lambda'_\ell = \{-1, -\lambda_1, \dots\}$. Then

$$(\mathbb{W} - \Pi)^{-1} = - \sum_{\ell=0}^{|\Omega|-1} \frac{1}{\lambda'_\ell} \boldsymbol{\psi}^{(\ell)} \otimes \boldsymbol{\phi}^{(\ell)} \quad (\text{B3a})$$

$$= -\Pi - \sum_{\ell=1}^{|\Omega|-1} \tau_\ell \boldsymbol{\psi}^{(\ell)} \otimes \boldsymbol{\phi}^{(\ell)}. \quad (\text{B3b})$$

The Drazin inverse of the rate matrix \mathbb{W} is thus

$$\mathbb{W}^{\mathcal{D}} = - \sum_{\ell=1}^{|\Omega|-1} \tau_{\ell} \psi^{(\ell)} \otimes \phi^{(\ell)}. \quad (\text{B4})$$

Appendix C: Drazin Inverse of the Fokker-Planck Operator

Here we show that the operator $\mathcal{L}^{\mathcal{D}}$ defined in (50) satisfies continuous analogs of the properties (26) and (23) of the Drazin inverse of a matrix. The spectral decomposition of a Fokker-Planck operator \mathcal{L} with a discrete spectrum and unique stationary distribution $\psi^{(0)}$ is

$$\mathcal{L}(x, y) = - \sum_{\ell=1}^{\infty} \lambda_{\ell} \psi^{(\ell)}(x) \phi^{(\ell)}(y). \quad (\text{C1})$$

By analogy to the spectral decomposition of the Drazin inverse of a matrix (44), define the Drazin inverse of \mathcal{L} :

$$\mathcal{L}^{\mathcal{D}}(x, y) = - \sum_{\ell=1}^{\infty} \tau_{\ell} \psi^{(\ell)}(x) \phi^{(\ell)}(y). \quad (\text{C2})$$

Composing \mathcal{L} with $\mathcal{L}^{\mathcal{D}}$ gives

$$\begin{aligned} (\mathcal{L} \circ \mathcal{L}^{\mathcal{D}})(x, y) &= \sum_{\ell, k} \frac{\tau_{\ell}}{\tau_j} \psi^{(\ell)}(x) \phi^{(k)}(y) \int_{\Omega} dz \phi^{(\ell)}(z) \psi^{(k)}(z) \quad (\text{C3a}) \\ &= \sum_{\ell=1}^{\infty} \psi^{(\ell)}(x) \phi^{(\ell)}(y), \quad (\text{C3b}) \end{aligned}$$

where the second step follows from the orthonormality of the eigenfunctions (5). Under the additional assumption that the eigenfunctions satisfy the completeness condition

$$\sum_{i=0}^{\infty} \psi^{(i)}(x) \phi^{(i)}(y) = \delta(x - y), \quad (\text{C4})$$

this further simplifies to

$$(\mathcal{L} \circ \mathcal{L}^{\mathcal{D}})(x, y) = \delta(x - y) - \psi^{(0)}(x). \quad (\text{C5})$$

Thus $\mathcal{L} \circ \mathcal{L}^{\mathcal{D}}$ is the deviation operator δ that maps p to $p - \pi \equiv \delta p$.

The properties $[\mathcal{L}, \mathcal{L}^{\mathcal{D}}] = 0$ and $\mathcal{L}^{\mathcal{D}} \psi^{(0)} = 0$ follow from the definition of \mathcal{L} and $\mathcal{L}^{\mathcal{D}}$. The remaining properties (23) follow straightforwardly:

$$\begin{aligned} (\mathcal{L} \circ \mathcal{L}^{\mathcal{D}} \circ \mathcal{L})(x, y) &= \int_{\Omega} dz \mathcal{L}(x, z) [\delta(z - y) - \pi(z)] \quad (\text{C6a}) \\ &= \mathcal{L}(x, y) - (\mathcal{L}\pi)(x) \quad (\text{C6b}) \\ &= \mathcal{L}(x, y). \quad (\text{C6c}) \end{aligned}$$

The proof that $\mathcal{L}^{\mathcal{D}} \circ \mathcal{L} \circ \mathcal{L}^{\mathcal{D}} = \mathcal{L}^{\mathcal{D}}$ is similar.

-
- [1] B. Andresen, Current trends in finite-time thermodynamics, *Angew. Chem., Int. Ed. Engl.* **50**, 2690 (2011).
 - [2] U. Seifert, Stochastic thermodynamics, fluctuation theorems, and molecular machines, *Rep. Prog. Phys.* **75**, 126001 (2012).
 - [3] A. I. Brown and D. A. Sivak, Theory of nonequilibrium free energy transduction by molecular machines, *Chem. Rev.* **120**, 434 (2020).
 - [4] S. Blaber and D. A. Sivak, Optimal control with a strong harmonic trap, *Phys. Rev. E* **106**, L022103 (2022).
 - [5] M. Esposito, R. Kawai, K. Lindenberg, and C. Broeck, Finite time thermodynamics for a single level quantum dot, *EPL* **89**, 20003 (2010).
 - [6] A. Zhong and M. R. DeWeese, Limited-control optimal protocols arbitrarily far from equilibrium, *Phys. Rev. E* **106**, 044135 (2022).
 - [7] T. Schmiedl and U. Seifert, Optimal finite-time processes in stochastic thermodynamics, *Phys. Rev. Lett.* **98**, 108301 (2007).
 - [8] J. Yan, H. Touchette, and G. M. Rotskoff, Learning nonequilibrium control forces to characterize dynamical phase transitions, *Phys. Rev. E* **105**, 024115 (2022).
 - [9] D. A. Sivak and G. E. Crooks, Thermodynamic metrics and optimal paths, *Phys. Rev. Lett.* **108**, 190602 (2012).
 - [10] D. A. Sivak and G. E. Crooks, Thermodynamic geometry of minimum-dissipation driven barrier crossing, *Phys. Rev. E* **94**, 052106 (2016).
 - [11] J. N. E. Lucero, A. Mehdizadeh, and D. A. Sivak, Optimal control of rotary motors, *Phys. Rev. E* **99**, 012119 (2019).
 - [12] D. Gupta, S. H. L. Klapp, and D. A. Sivak, Efficient control protocols for an active Ornstein-Uhlenbeck particle, *Phys. Rev. E* **108**, 024117 (2023).
 - [13] S. Tafuya, S. J. Large, S. Liu, C. Bustamante, and D. A. Sivak, Using a system's equilibrium behavior to reduce its energy dissipation in nonequilibrium processes, *Proc. Natl. Acad. Sci.* **116**, 5920 (2019).
 - [14] S. Blaber and D. A. Sivak, Efficient two-dimensional control of barrier crossing, *EPL* **139**, 17001 (2022).
 - [15] J.-F. Chen, R.-X. Zhai, C. P. Sun, and H. Dong, Geodesic lower bound of the energy consumption to achieve membrane separation within finite time, *PRX Energy* **2**, 033003 (2023).
 - [16] S. Deffner, Kibble-Zurek scaling of the irreversible en-

- tropy production, Phys. Rev. E **96**, 052125 (2017).
- [17] P. R. Zulkowski and M. R. DeWeese, Optimal protocols for slowly driven quantum systems, Phys. Rev. E **92**, 032113 (2015).
- [18] V. Lindahl, J. Lidmar, and B. Hess, Riemann metric approach to optimal sampling of multidimensional free-energy landscapes, Phys. Rev. E **98**, 023312 (2018).
- [19] M. Lundborg, J. Lidmar, and B. Hess, On the path to optimal alchemy, Protein J. **42**, 477 (2023).
- [20] L. P. Kamizaki, M. V. S. Bonança, and S. R. Muniz, Performance of optimal linear-response processes in driven Brownian motion far from equilibrium, Phys. Rev. E **106**, 064123 (2022).
- [21] P. Salamon and A. Nitzan, Finite time optimizations of a Newton's law Carnot cycle, J. Chem. Phys. **74**, 3546 (1981).
- [22] B. Remlein and U. Seifert, Optimality of nonconservative driving for finite-time processes with discrete states, Phys. Rev. E **103**, L050105 (2021).
- [23] G. M. Rotskoff, G. E. Crooks, and E. Vanden-Eijnden, Geometric approach to optimal nonequilibrium control: Minimizing dissipation in nanomagnetic spin systems, Phys. Rev. E **95**, 012148 (2017).
- [24] K. Brandner and K. Saito, Thermodynamic geometry of microscopic heat engines, Phys. Rev. Lett. **124**, 040602 (2020).
- [25] D. Mandal and C. Jarzynski, Analysis of slow transitions between nonequilibrium steady states, J. Stat. Mech.: Theory Exp. **2016** (6), 063204.
- [26] V. V. Prasolov, *Differential geometry* (Cham, Switzerland : Springer, 2022).
- [27] R. M. Wald, *General relativity* (Chicago : University of Chicago Press, 1984).
- [28] P. R. Zulkowski and M. R. DeWeese, Optimal finite-time erasure of a classical bit, Phys. Rev. E **89**, 052140 (2014).
- [29] A. G. Frim and M. R. DeWeese, Optimal finite-time Brownian Carnot engine, Phys. Rev. E **105**, L052103 (2022).
- [30] P. R. Zulkowski and M. R. DeWeese, Optimal control of overdamped systems, Phys. Rev. E **92**, 032117 (2015).
- [31] G. M. Rotskoff and G. E. Crooks, Optimal control in nonequilibrium systems: Dynamic Riemannian geometry of the Ising model, Phys. Rev. E **92**, 060102 (2015).
- [32] M. D. Louwse and D. A. Sivak, Multidimensional minimum-work control of a 2D Ising model, J. Chem. Phys. **156**, 194108 (2022).
- [33] A. Ben-Israel, *Generalized Inverses: Theory and Applications*, edited by T. N. E. Greville (Wiley, New York, 1974).
- [34] P. M. Riechers and J. P. Crutchfield, Beyond the spectral theorem: Spectrally decomposing arbitrary functions of nondiagonalizable operators, AIP Adv. **8**, 065305 (2018).
- [35] N. G. Van Kampen, The Master Equation, in *Stochastic Processes in Physics and Chemistry (Third Edition)* (Elsevier, Amsterdam, 2007) pp. 96–133.
- [36] G. E. Crooks, On the Drazin inverse of the rate matrix (2018).
- [37] M. Scandi and M. Perarnau-Llobet, Thermodynamic length in open quantum systems, Quantum **3**, 197 (2019).
- [38] H. J. D. Miller, M. Scandi, J. Anders, and M. Perarnau-Llobet, Work fluctuations in slow processes: Quantum signatures and optimal control, Phys. Rev. Lett. **123**, 230603 (2019).
- [39] D. D. Yao, First-passage-time moments of markov processes, J. Appl. Probab. **22**, 939 (1985).
- [40] P. Coolen-Schrijner and E. A. van Doorn, The deviation matrix of a continuous-time Markov chain, Probab. Eng. Inf. Sci. **16**, 351 (2002).
- [41] G. A. Pavliotis, *Stochastic Processes and Applications: Diffusion Processes, the Fokker-Planck and Langevin Equations*, Vol. 60 (Springer Nature, New York, 2014).
- [42] H. Risken, *The Fokker-Planck Equation : Methods of Solution and Applications*, 2nd ed., edited by T. Frank (Springer Berlin Heidelberg, 1996).
- [43] J. Liphardt, S. Dumont, S. B. Smith, I. Tinoco, and C. Bustamante, Equilibrium information from nonequilibrium measurements in an experimental test of Jarzynski's equality, Science **296**, 1832 (2002).
- [44] D. Collin, F. Ritort, C. Jarzynski, S. B. Smith, I. Tinoco, and C. Bustamante, Verification of the Crooks fluctuation theorem and recovery of RNA folding free energies, Nature **437**, 231 (2005).
- [45] S. Blaber and D. A. Sivak, Optimal control in stochastic thermodynamics, J. Phys. Commun. **7**, 033001 (2023).
- [46] Maplesoft, a division of Waterloo Maple Inc., Waterloo, Ontario., Maple 2024.
- [47] It is trivially true that $\mathcal{N}(\mathbb{J}^T) \subseteq \mathcal{N}(\mathbb{J}\mathbb{J}^T)$. $\mathcal{N}(\mathbb{J}\mathbb{J}^T) \subseteq \mathcal{N}(\mathbb{J}^T)$ is shown as follows: $\mathbb{J}\mathbb{J}^T \mathbf{v} = 0 \implies \mathbf{v}^T \mathbb{J}\mathbb{J}^T \mathbf{v} = (\mathbb{J}^T \mathbf{v})^2 = 0 \implies \mathbf{v} \in \mathcal{N}(\mathbb{J}^T)$.
- [48] A. Brøndsted, *An Introduction to Convex Polytopes*, Graduate Texts in Mathematics, Vol. 90 (Springer, New York, NY, 1983).